

# Spontaneously grown GaN and AlGaN nanowires<sup>☆</sup>

K.A. Bertness<sup>a,\*</sup>, A. Roshko<sup>a</sup>, N.A. Sanford<sup>a</sup>, J.M. Barker<sup>a</sup>, A.V. Davydov<sup>b</sup>

<sup>a</sup>National Institute of Standards and Technology, Mail Stop 815.04, 325 Broadway, Boulder, CO 80305, USA

<sup>b</sup>National Institute of Standards and Technology, 100 Bureau Drive, Stop 8555, Gaithersburg, MD 20899-8555, USA

Available online 4 January 2006

## Abstract

We have identified crystal growth conditions in gas-source molecular beam epitaxy (MBE) that lead to spontaneous formation of GaN nanowires with high aspect ratio on Si (1 1 1) substrates. The nanowires were oriented along the GaN *c*-axis and normal to the substrate surface. Unlike in many other reports of GaN nanowire growth, no metal catalysts were used. Low growth rates at substrate temperatures near 820 °C were combined with high nitrogen flux (partially dissociated with RF plasma excitation) to form well-separated GaN wires with diameters from 50 to 250 nm in diameter and lengths ranging from 2 to 7 μm. The nanowires grew out of an irregular matrix layer containing deep faceted holes. X-ray diffraction indicated that the wires were fully relaxed and aligned to the silicon substrate. The growth morphology was strongly affected by the presence of Al and Be. The changes suggest that surface diffusion is a primary driving force in the growth of GaN nanowires with MBE.

Published by Elsevier B.V.

PACS: 81.07.Bc; 81.15.Hi; 81.05.Ea; 68.37.Hk; 68.35.Ct

Keywords: A1. Nanostructures; A3. Molecular beam epitaxy; B1. Nitrides; B2. Semiconducting III–V materials

## 1. Introduction

GaN nanowires are promising for a number of technical applications because they enable the growth of high-quality material on inexpensive substrates, in this case silicon wafers. There is also the opportunity to integrate the nanowires with silicon circuitry, either through direct growth or with post-processing placement of wires. The wires themselves are similar in size to the active regions of many lasers, LEDs and transistors. A number of groups have reported device results with GaN nanowires formed using catalytic growth in which small metal droplets, most commonly nickel or gold, are first formed on the surface. The metal droplets enable the growth through the vapor–liquid–solid (VLS) mechanism to form long wires with approximately the diameter of the droplet. These VLS wires vary in their crystal orientation and in their tendency

to tilt, twist, intersect, and branch during growth. Catalyst-grown nanowires have been shown to achieve stimulated emission under pulsed optical pumping [1], light emission from p–n junctions [2], and gated transistor behavior [3]. Nanowire growth has also been demonstrated with seeded growth, in which small GaN crystals are intentionally formed at the beginning of the growth process. Seeded-growth LEDs have been manufactured from p–n junction nanowires grown with hydride vapor phase epitaxy (HVPE) [4] and molecular beam epitaxy (MBE) [5].

We have identified crystal growth conditions in gas-source MBE that lead to spontaneous formation of GaN nanowires with high aspect ratio and high luminescent efficiency. The nanowires grew normal to the surface of the substrate material, Si (1 1 1), with hexagonal cross-sections and oriented along the GaN *c*-axis. Wires ranged from 50 to 250 nm across, and were grown in lengths ranging from 2 to 7 μm long. Unlike most other reports of GaN nanowires, no metal catalysts were used. Our analysis of the spontaneous formation of the nanowires suggests that surface diffusion kinetics were primarily responsible for the formation of the nanowires, although a detailed

<sup>☆</sup>Contribution of an agency of the U.S. Government; not subject to copyright.

\*Corresponding author. Tel.: +1 303 497 5069; fax: +1 303 497 3387.

E-mail address: [bertness@boulder.nist.gov](mailto:bertness@boulder.nist.gov) (K.A. Bertness).

mechanism has not yet been determined. Consistent with the limited work on catalyst-free growth of GaN nanowires in MBE [6], the flux ratio of group V element (N) to group III elements (Ga and Al) has a significant influence on the growth morphology. The relationship is not a simple one, however, possibly due to the complex set of nitrogen species produced by a radio-frequency (RF) plasma. We further observe that Al and Be significantly alter the growth morphology. Both elements are known to affect average group III surface diffusion in the epitaxial growth of other III–V materials, and hence we would expect them to alter surface diffusion in nanowires as well.

The nanowire characteristics imply a high probability of success for electronic and optoelectronic device development. The wires were readily dispersed onto other substrates (such as sapphire and silicon) by placing as-grown specimens in solvents under ultrasonic agitation, dispensing droplets of the slurry onto a new substrate, and allowing the solvent to evaporate. Unpolarized photoluminescence at 3 K from both as-grown and dispersed samples showed the donor-bound exciton peak near  $3.472 \pm 0.0005$  eV dominating the spectrum, with intensities comparable to a reference sample of free-standing, HVPE GaN under equivalent excitation conditions. The high luminescent efficiency and the observation of phonon replicas is an indicator of the relatively low defect density in the nanowires. The  $c$  and  $a$  lattice parameters of the nanowires were within 0.02% and 0.07%, respectively, of the bulk GaN crystal values [7]. In agreement with other work on GaN nanowires [8,9], TEM data confirmed that these nanowires were free of visible defects. Additional details of the electrical and optical properties will be discussed in future publications.

## 2. Experimental procedure

The nanowire growths took place in a conventional gas-source MBE system with Knudsen cell Ga, Al, Si, and Be sources and an RF plasma N source. We report both the nitrogen flow and RF plasma power for the N source; the most typical operating conditions during GaN nanowire growth were  $2.1 \mu\text{mol/s}$  (3 sccm) and 450 W, respectively. The external RF impedance matching circuit was adjusted so that the reflected power was less than 12 W. Substrate temperature measurements were made using an optical pyrometer, which yielded measurements with an expanded uncertainty of approximately  $8^\circ\text{C}$ . Silicon (111) wafers were prepared for growth with a 90 s etch in a 10% HF:H<sub>2</sub>O mixture by volume, rinsed for a few seconds in static deionized water, and blown dry with a filtered nitrogen gun. The wafers were outgassed in a preparation chamber to  $750 \pm 15^\circ\text{C}$  for 15 min, then outgassed again at  $850^\circ\text{C}$  for 10 min in the growth chamber. Following standard procedures developed for the growth of GaN on silicon [10,11], we first deposited a 0.5 nm layer of pure Al at  $700^\circ\text{C}$ , then grew 50–80 nm of AlN at a growth temperature of  $630^\circ\text{C}$ . The nanowires were typically grown

at a substrate temperature of  $820^\circ\text{C}$ . Ga flux was measured using an ion gauge placed just in front of the substrate manipulator; beam equivalent pressures were  $1.3 \times 10^{-5}$  Pa ( $1.0 \times 10^{-7}$  Torr) for low flux and  $2.1\text{--}2.4 \times 10^{-5}$  Pa for medium flux conditions. Beam flux measurements had an uncertainty of about 10%. The V:III ratios in this paper were calculated by taking the ratio of the Ga beam equivalent pressure and the nitrogen pressure in the chamber.

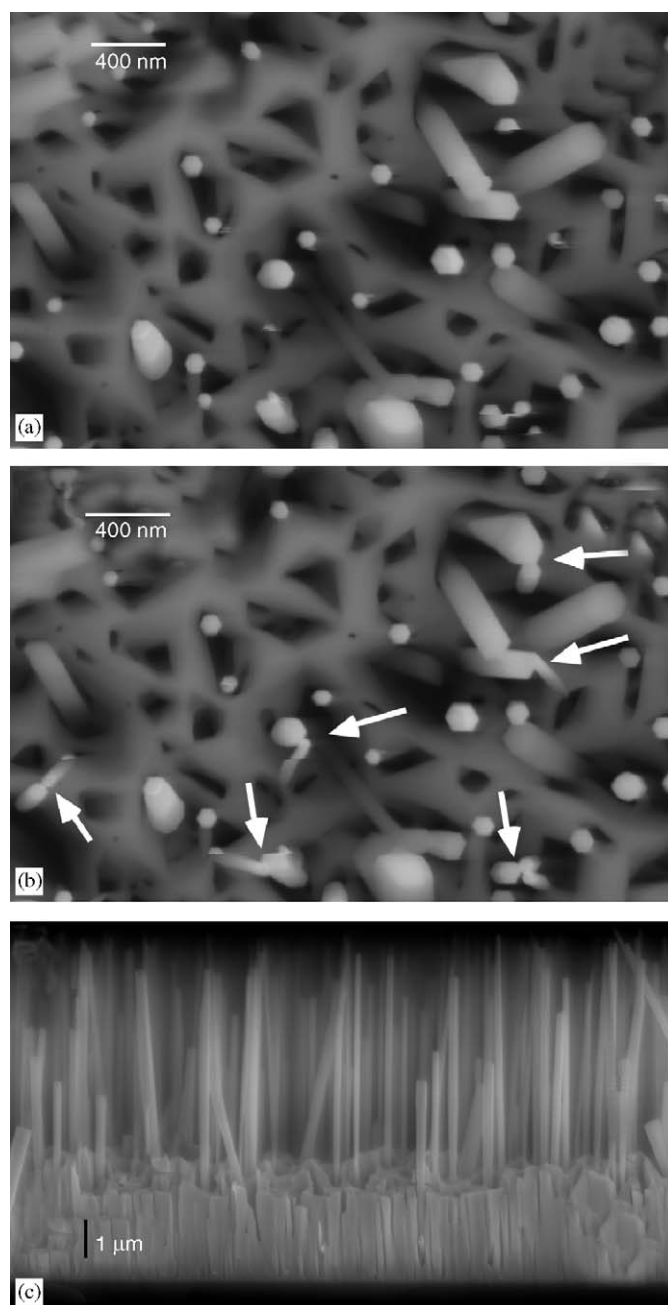


Fig. 1. Plan view (a) and (b) and cross-section view (c) of typical GaN nanowire growth on silicon, illustrating the aligned, hexagonal cross-sections and straight side-walls. (a) and (b) were acquired sequentially with a time separation of approximately 2 min, during which time charging from the electron beam caused some wires to move together (indicated with arrows).

### 3. Results and discussion

The basic morphology of the GaN nanowires is illustrated by the field emission scanning electron microscopy (FESEM) images in Fig. 1. The wires exhibited highly symmetric hexagonal cross-sections with widths ranging from 50 to 150 nm in this sample. The hexagonal wires were also aligned to each other, an indication that they take their crystallographic orientation from the underlying silicon substrate. The wires were straight as grown, with no tilt visible in the plan view FESEM image despite wire aspect ratios of up to 50:1. The wires became electrostatically charged under high electron beam currents, however, and would bend toward one another as illustrated by the arrows in Fig. 1(b). X-ray diffraction confirms that the wires were oriented with the growth direction along the *c*-axis of the GaN. The hexagonal facets conform to  $\{10\bar{1}0\}$  planes. The GaN nanowires from this

specimen extend 2.5  $\mu\text{m}$  beyond the irregular matrix layer through which they grow (Fig. 1(c)). The nanowire roots were frequently observed to extend deep into the matrix layer, and for specimens with well-separated nanowires such as these, the wires grew at roughly twice the rate as the matrix. Although occasional nucleation of nanowires on top of the matrix or other larger structures was observed, most nanowires appeared to nucleate early in the growth process.

As discussed in the introduction, the morphology of the wires was expected to be strongly affected by V:III ratio. Figs. 2 and 3 display SEM images from a series of four growth runs varying the nitrogen flow rate and RF plasma power. Medium Ga flux and growth temperatures in the range 810–820 °C were used for these runs, and the two nitrogen flow rates were 2.1 and 0.7  $\mu\text{mol/s}$ . The matrix morphology was very similar for runs with similar V:III ratio, but the density and length of the nanowires was

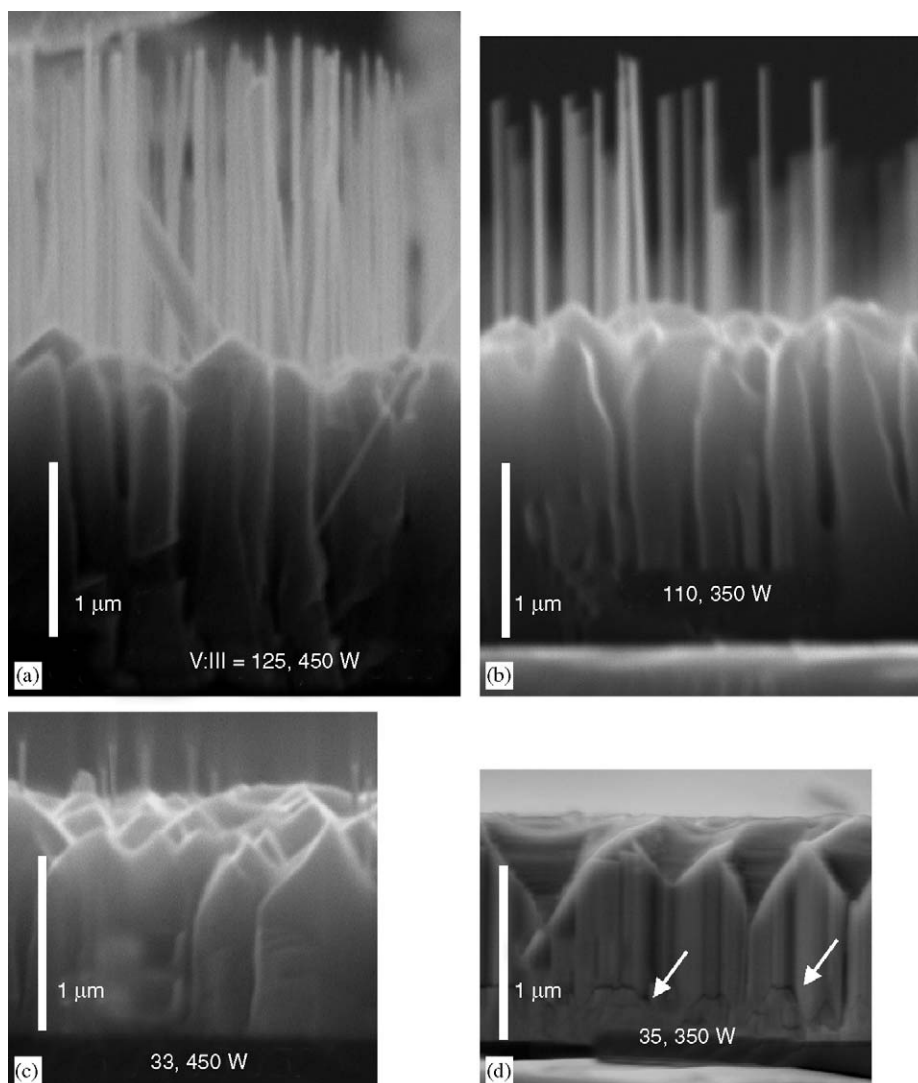


Fig. 2. Cross-section SEM images of GaN nanowire samples with varying V:III ratio and RF plasma power, as shown. An AlN marker layer (arrows) is visible in (d), showing the surface faceting structure was established early in the growth.

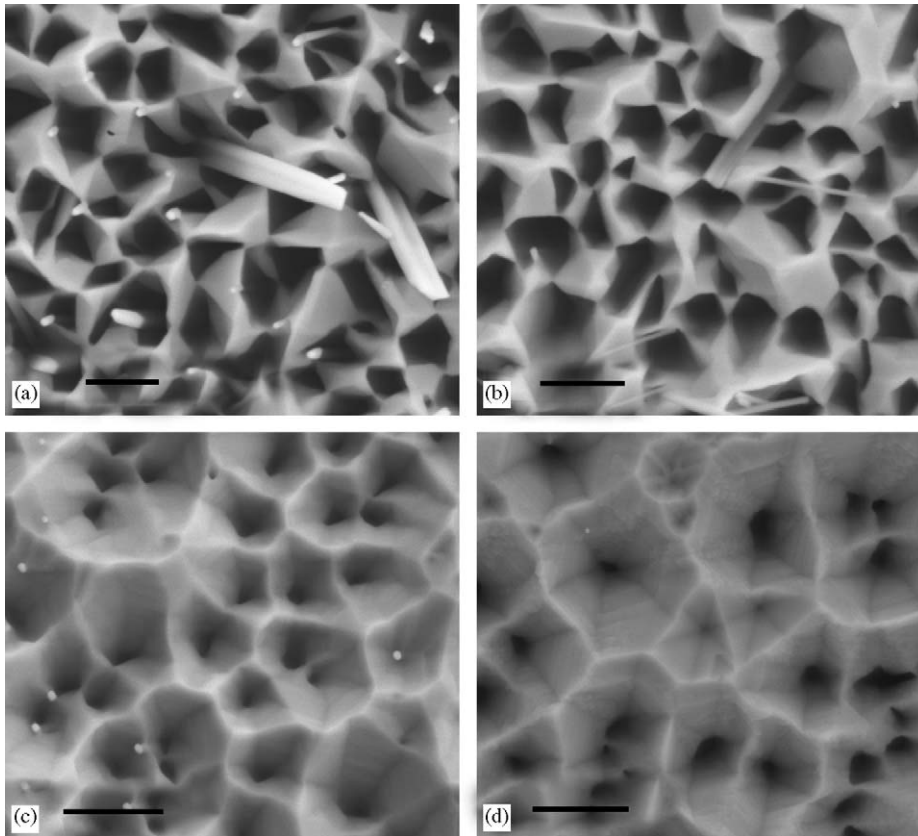


Fig. 3. Plan-view FESEM images of GaN nanowire samples with varying V:III ratio and RF plasma power as (a) 125, 450 W; (b) 110, 350 W; (c) 33, 450 W and (d) 35, 350 W. The marker bars represent 1  $\mu\text{m}$ .

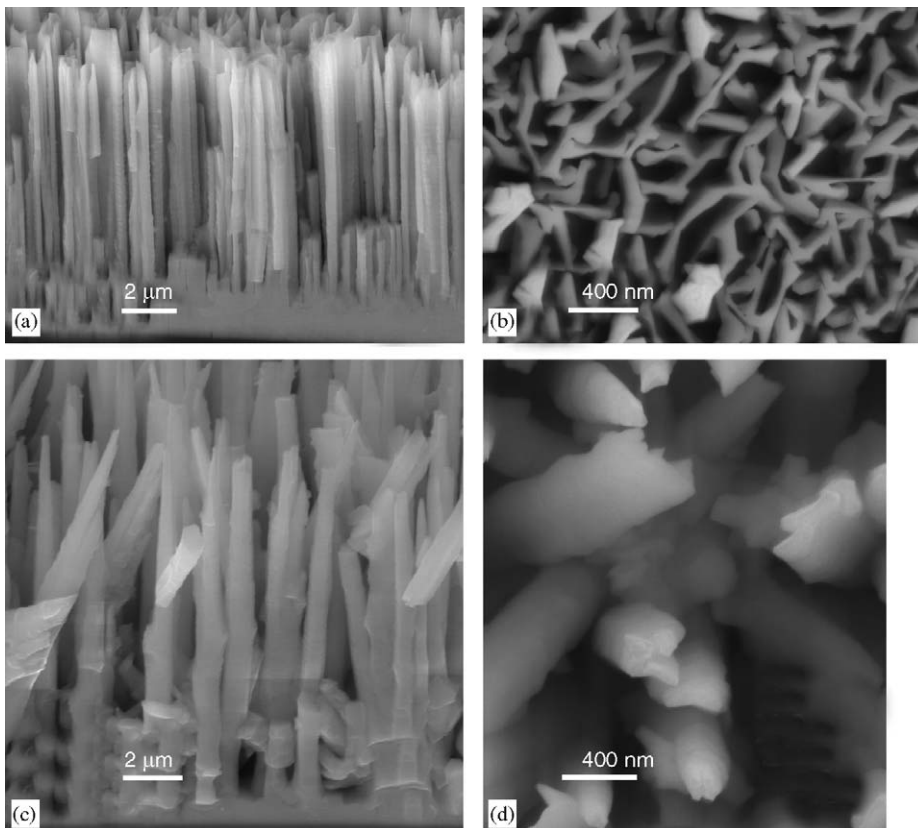


Fig. 4. Effect of Be flux on nanowire growth. Be concentration was approximately  $1 \times 10^{20} \text{ cm}^{-3}$  in (a) and (b), with V:III = 145, and  $5 \times 10^{19} \text{ cm}^{-3}$  in (c) and (d), with V:III = 170. (a) and (c) were taken with the substrate tilted  $40^\circ$  and  $30^\circ$ , respectively, from an edge-on view.

noticeably enhanced at higher plasma power. The change in the matrix layer morphology suggests an enhancement of atomic diffusion in the vertical direction as the V:III ratio and plasma power increase. This process is also thermally activated, as indicated by an additional sample (not shown) grown with substrate temperature of approximately 760 °C. At the lower temperature, both the deep facets and nanowires did not form.

Although these results agree qualitatively with those of Calleja et al., the quantitative agreement is poor. This group reports nanowire formation [6,12,13] at lower temperatures (760 °C) and higher Ga flux ( $>7 \times 10^{-5}$  Pa) with lower nitrogen flow (0.7  $\mu\text{mol/s}$ ) and similar RF power (400–580 W). The nanowires were not generally as isolated as the ones we have illustrated in Fig. 1, and the reported morphologies never resembled Figs. 2(c), (d), 3(c) and (d). Possible explanations for these discrepancies include variations in nitrogen active species, growth temperature calibration, and buffer layers [14].

The mechanism of nanowire growth in MBE is not well-established. In analogy to metal-catalyst growth, the VLS mechanism [6] has been proposed with Ga droplets playing the role of the metal catalyst. Because residual droplets have never been observed on the nanowire tips, and droplet formation is unfavorable under nitrogen-rich conditions, we propose instead that differential surface diffusion is more likely to be the main driving force. Specifically, diffusion of group III atoms along the vertical crystal planes may become very rapid for some growth conditions [15], while diffusion across the top surfaces is relatively slower, leading to greater incorporation on the top surface. Surface diffusion is expected to increase on all surfaces with increasing temperature and to be lower for Al than for Ga. Be, which tends to surface segregate in other III–V alloys, might also be expected to enhance diffusion. High group V pressure typically reduces group III diffusion coefficients; however, the effect could be strongly dependent on the surface configuration, and in particular might be largest for polar surfaces such as the top plane of the nanowires.

The morphology of Be-doped GaN wires and AlGaN wires in Figs. 4 and 5 support a model in which diffusion in the vertical direction is enhanced by Be and suppressed by Al. In Fig. 4, increasing Be flux with only small variations in other growth conditions led to transformation of the entire matrix layer into large vertical ribbons, some of which had slightly conical shape (Fig. 4(d)). The sidewalls of the vertical ribbons in Fig. 4(a) are roughly aligned with  $\{10\bar{1}0\}$  planes, the same planes that comprise the sidewalls of the hexagonal nanowires. This plane is one of the more stable surfaces of GaN, being nonpolar and having a high atomic density. It is therefore not surprising that the surface diffusion coefficient of adatoms might be high, particularly at high temperatures.  $\text{Al}_x\text{Ga}_{1-x}\text{N}$  nanowires (with  $x$  between 0.2 and 0.4) grew progressively thicker with length and finally coalesced after a few micrometers of length (Fig. 5). Increasing the growth temperature by 20 °C

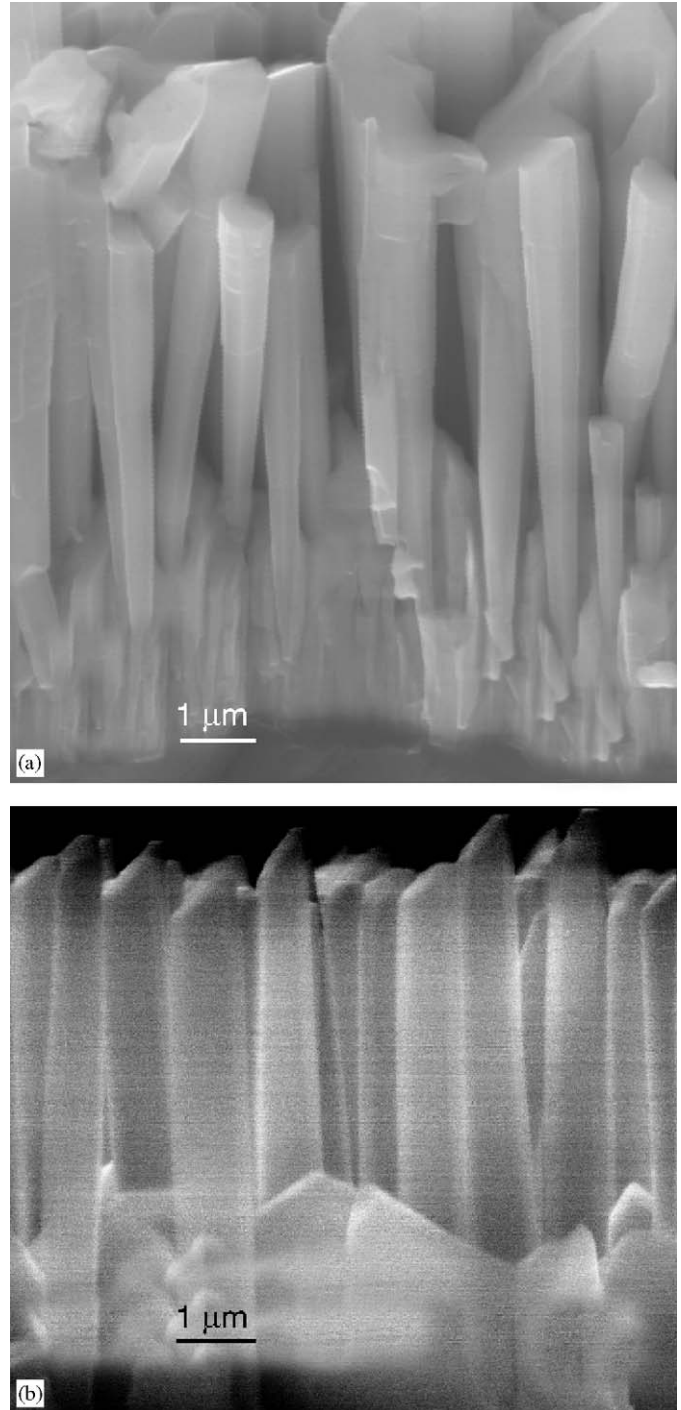


Fig. 5. FESEM images of AlGaN nanowires illustrating the tendency of the wires to thicken and coalesce and to terminate in tilted planes. The nominal Al mole fractions of the AlGaN sections are 0.2 and 0.3 in (a) and (b), respectively. The specimen in (a) was tilted 30° relative to edge-on during imaging.

was insufficient to maintain isolated wire growth. The higher bond strength of Al–N relative to Ga–N explains this variation through a probable reduction in surface diffusion coefficient. The isolated AlGaN nanowires in Fig. 5(b) were obtained by initiating growth with GaN and

then stopping growth before the wires grew beyond 1  $\mu\text{m}$  in length. Another interesting aspect of the AlGaN nanowires was their tendency to terminate in planes tilted approximately  $60^\circ$  from the wire axis. While the variation in this angle was too large for a definitive identification, we tentatively associate these surfaces with  $\{10\bar{1}3\}$  planes.

#### 4. Summary

GaN and AlGaN nanowires have been grown with low defect density on Si(111) using MBE. The wires form spontaneously under growth conditions that promote differential surface diffusion on the different planes comprising the sides and tops of the wires. The same conditions that promote wire growth also lead to increased vertical growth in the matrix layer beneath the wires. Specifically, the matrix layer transformed into mostly vertical ribbons and cones when Be was added as a surfactant, and adding Al resulted in increasing wire diameter during growth. Because the growth conditions used in these experiments differed quantitatively from conditions reported by other groups, the nanowire formation mechanism appears to depend on additional parameters not yet identified.

#### References

- [1] J.C. Johnson, H.-J. Choi, K.P. Knutsen, R.D. Schaller, P. Yang, R.J. Saykally, *Nat. Mater.* 1 (2002) 106.
- [2] Z. Zhong, F. Qian, D. Wang, C.M. Lieber, *Nano Lett.* 3 (2003) 343.
- [3] M.C. McAlpine, R.S. Friedman, S. Jin, K.-H. Lin, B. Wang, W.U., C.M. Lieber, *Nano Lett.* 3 (2003) 1531.
- [4] H.-M. Kim, T.W. Kang, K.S. Chung, *Adv. Mater.* 15 (2003) 567.
- [5] A. Kikuchi, M. Kawai, M. Tada, K. Kishino, *Jpn. J. Appl. Phys. Part 2* 43 (2004) L1524.
- [6] E. Calleja, M.A. Sánchez-García, F.J. Sánchez, F. Calle, F.B. Naranjo, E. Muñoz, U. Jahn, K. Ploog, *Phys. Rev. B* 62 (2000) 16826.
- [7] S. Porowski, *J. Crystal Growth* 190 (1998) 153.
- [8] Y. Inoue, T. Hoshino, S. Takeda, K. Ishino, A. Ishida, H. Fujiyasu, H. Kominami, H. Mimura, Y. Nakanishi, S. Sakakibara, *Appl. Phys. Lett.* 85 (2004) 2340.
- [9] J. Ristic, E. Calleja, M.A. Sanchez-Garcia, J.M. Ulloa, J. Sanchez-Paramo, J.M. Calleja, U. Jahn, A. Trampert, K.H. Ploog, *Phys. Rev. B* 68 (2004) 125305-1.
- [10] S.A. Nikishin, V.G. Antipov, S. Francoeur, N.N. Faleev, G.A. Seryogin, V.A. Elyukhin, H. Temkin, T.I. Prokofyeva, M. Holtz, A. Konkar, S. Zollner, *Appl. Phys. Lett.* 75 (1999) 484.
- [11] R. Liu, F.A. Ponce, A. Dadgar, A. Krost, *Appl. Phys. Lett.* 83 (2003) 860.
- [12] J. Ristic, M.A. Sanchez-Garcia, E. Calleja, J. Sanchez-Paramo, J.M. Calleja, U. Jahn, K.H. Ploog, *Phys. Status Solidi A* 192 (2002) 60.
- [13] M.A. Sanchez-Garcia, E. Calleja, E. Monroy, F.J. Sanchez, F. Calle, E. Munoz, R. Beresford, *J. Crystal Growth* 183 (1998) 23.
- [14] K.A. Bertness, A. Roshko, N.A. Sanford, J.B. Schlager, M.H. Gray, *Phys. Stat. Sol. (c)* 2 (2005) 2369.
- [15] C.Y. Nam, D. Tham, J.E. Fischer, *Appl. Phys. Lett.* 85 (2004) 5676.